Hydrogen solubility and network stability in amorphous silicon

S. Acco
Debye Institute, Utrecht University, P.O. Box 80000, 3508 TA Utrecht, The Netherlands and FOM-Institute for Atomic and Molecular Physics, Kruislaan 407, 1098 SJ Amsterdam, The Netherlands

D. L. Williamson
Department of Physics, Colorado School of Mines, Golden, Colorado 80401

P. A. Stolk
AT&T Bell Laboratories, 600 Mountain Avenue, Murray Hill, New Jersey 07974

F. W. Saris
FOM-Institute for Atomic and Molecular Physics, Kruislaan 407, 1098 SJ Amsterdam, The Netherlands

M. J. van den Boogaard, W. C. Sinke,* and W. F. van der Weg
Debye Institute, Utrecht University, P.O. Box 80000, 3508 TA Utrecht, The Netherlands

S. Roorda
Group de Recherche en Physique et Technologie des Couches Minces, Départment de Physique, Université de Montréal, Case Postale 6128 Succursale Centre-ville, Montréal, QC H3C Canada

P. C. Zalm
Philips Research Laboratories, Prof. Holstlaan 4, 5656 AA Eindhoven, The Netherlands
(Received 14 September 1995)

In order to investigate the role of hydrogen in amorphous silicon (*a*-Si), hydrogenated amorphous silicon layers have been prepared by ion implantation at different H concentrations. Implanted samples have been characterized before and after annealing up to 550 °C by small-angle x-ray scattering, secondary-ion-mass spectrometry, and infrared spectroscopy. The study of the evolution of hydrogen concentration profiles and bonding configurations combined with the investigation of the atomic and nanoscale structures of the films indicate the solubility limit of hydrogen in *a*-Si to lie at 3–4 at. %. This limit is associated with the defect-related trap concentration in *a*-Si. If hydrogen is introduced in the matrix at a concentration well above its solubility, the alloy is intrinsically unstable to the formation of hydrogen complexes. Upon annealing at temperatures higher than 300 °C, the excess H (i.e., above the solubility) leaves the matrix, presumably forming H_2 molecules, which accumulate in nanoscale hydrogen complexes. Observations on nucleation and growth of these hydrogen complexes are discussed in light of H diffusion and solubility.

I. INTRODUCTION

One of the important issues concerning the interaction of hydrogen with the Si bulk in hydrogenated amorphous silicon (*a*-Si:H) is the role that hydrogen plays in structural-defect formation. Presently, *a*-Si:H films are deposited by a variety of techniques such as plasma-enhanced chemical vapor deposition (PECVD), rf sputtering, and hot-filament CVD. Hydrogenated amorphous silicon obtained by deposition is not homogeneous, but contains low-density inhomogeneities with typical sizes of 1–10 nm, embedded in the amorphous matrix.[1–3] These features are thought to be voids or H-rich clusters, and it has been suggested that their presence decreases the local strain of the *a*-Si network.[4] Since these structural defects may be detrimental to the optoelectronic properties of the film, voids have been extensively investigated in the past few years. Films of poor electronic quality may have void contents of several vol.%,[2,5–7] while in device-quality material contents are usually near or well below 1 vol.%.[5–10] The void density is affected by thermal-annealing treatments subsequent to deposition, and has been seen to increase during annealing at temperatures over ∼300 °C in the case of rf-sputtered and good-quality PECVD films.[11,12]

The morphology of the material depends strongly on growth conditions.[2,7,9,13] Changes in the hydrogen concentration [H] have been observed to affect the void content and films with [H]⩾15 at. % appear inhomogeneous, almost regardless of the preparation method.[14,15] On the other hand, recent experiments have shown that *a*-Si:H requires only a few at. % of hydrogen to be of high quality.[16–18] A clear understanding of the relationship between nanovoids and [H] is, however, still lacking, mostly because, in deposited films, it is not possible to distinguish unambiguously the influence of the deposition conditions from the role of hydrogen itself.

In the past decade, many studies have been made of pure (i.e., unhydrogenated) *a*-Si produced by ion implantation.[19] This material has properties that are insensitive to the prepa-

0163-1829/96/53(8)/4415(13)/$06.00 © 1996 The American Physical Society

ration details, suggesting that the structure is independent of the implantation parameters. Its investigation has provided useful information on the silicon matrix that constitutes the rigid frame of the a-Si:H network. The defect density in the as-implanted state of a-Si has been estimated to be of the order of 1%. Heat treatments induce structural relaxation and decrease the defect concentration by a factor $\sim$4–5 with respect to the as-implanted state.[20,21] Ion-implanted a-Si is 1.8% less dense than c-Si,[22] and the changes in density observed during structural relaxation do not exceed 0.1%.[23] Furthermore, very recent small-angle x-ray scattering (SAXS) measurements have demonstrated the absence of nanovoids, within a sensitivity of 0.1 vol.%, both in the as-implanted and in the relaxed state of a-Si.[24]

The reproducibility and structural homogeneity of ion-implanted a-Si make this material particularly suitable as a system for the further investigation of the structural properties of hydrogen in a-Si. In the present work, we have implanted hydrogen into a-Si prepared by ion implantation [a-Si(H)] with the objective of investigating the interaction between H and the a-Si network. The atomic and nanoscale structures, the concentration and evolution of hydrogen, and the hydrogen bonding were studied using small-angle x-ray scattering (SAXS), secondary-ion mass spectrometry (SIMS), and infrared (IR) spectroscopy, respectively. These experiments provide further insights on the nucleation and growth of hydrogen complexes in hydrogenated a-Si and our observations are discussed in light of H diffusion and solubility. Annealing of a homogeneous a-Si network structure, containing more than 10 at. % hydrogen, leads to the separation of the structure into a two-phase system: hydrogen dissolved in the a-Si matrix and hydrogen clustered in low-density inhomogeneities. The present studies demonstrate that inhomogeneities are caused by hydrogen complex formation.

Experimental details of sample preparation and characterization techniques are described in Sec. II. Results are presented in Sec. III, and Sec. IV reports the analysis in order to interpret the SAXS data quantitatively. A discussion follows in Sec. V, while in Sec. VI the correlation between diffusivity and solubility of H in a-Si and the clustering process are described. Conclusions are drawn in Sec. VII.

II. EXPERIMENT

A. Sample preparation

Two samples were prepared for SAXS measurements by self-ion bombardment at various ionization states with energies ranging from 0.5 to 17 MeV into 75-μm-thick double-polished Si wafers. The thickness of the a-Si layers produced was measured by Fourier-transform IR reflectivity measurements to be $\sim$8 μm for both samples. Hydrogen was introduced by implanting H_2^+ at energies ranging from 50 to 500 keV/amu. All H implants were performed with the Si targets held at $\sim$77 K by means of a liquid-nitrogen-cooled holder in order to improve vacuum conditions and avoid self-annealing processes. The resulting hydrogenated layer was measured by SIMS to be $\sim$6.5 μm. The implantation schedule was designed in order to achieve a hydrogenated amorphous layer sufficiently thick to detect the weak SAXS signals which were expected if low densities of inhomogeneities were present in the films.[24] The high-H content sample, designated as the HH sample, received a total fluence of 3.00×10^{18} cm^{-2} (corresponding to an average concentration of 8.5 at. % over the 6.5-μm layer) with a SIMS-determined average peak concentration of 20 at. % due to the nonuniform, as-implanted distribution. In the low-H content sample, designated as the LH sample, the injected dose was 3.7×10^{17} cm^{-2} (corresponding to an average H concentration of 1.1 at. %) with peak concentrations of 3–4 at. %, again due to the nonuniform, as-implanted state.

For SIMS and IR experiments, a single-crystal float-zone (FZ) silicon wafer was irradiated with Si^+ ions at energies of 0.5 and 1.0 MeV to a total dose of 5×10^{15} cm^{-2}. These implants produced a surface amorphous layer of 1.3–1.4-μm thickness. Samples were then implanted with H_2^+ at three different energies, 30, 50, and 80 keV/amu. The injected doses were estimated from effusion measurements to be 5.4×10^{17} cm^{-2} in the HH sample (20-at. % peak concentration) and 9.4×10^{16} cm^{-2} in the LH sample (4-at. % peak concentration), with an accuracy of a few percent. It is to be noted that doses were chosen in order to have H peak concentrations similar to those in the SAXS samples (HH and LH), and thus to allow comparison of results from the various techniques.

Samples were subsequently annealed at temperatures ranging from 200 to 550 °C. The anneal time was 4 h for all temperatures and anneals were done in 50 °C increments from 200–400 °C, and in 25 °C increments for higher temperatures. Anneals of the SAXS samples were made under high-purity, flowing He in a tube furnace, while anneals of the SIMS samples were performed in a vacuum furnace (pressure $\sim10^{-7}$ mbar). The different ambient conditions are not expected to have changed the bulk annealing behavior of the samples.

B. Characterization techniques

Secondary-ion mass spectrometry (SIMS). SIMS measurements were carried out using a Cameca IMS-4F ion microprobe with a sample chamber vacuum of 2×10^{-8} Torr during operation. With these vacuum conditions, the detection limit of H in Si was 2×10^{20} cm^{-3}. A 5.5-keV O_2^+ beam was scanned over a 175×175-μm^2 area and the intensities of $^{28}Si^{2+}$ and H^+ ions sputtered from the 30-μm-diameter center of the crater were monitored. The depth scale has a typical accuracy of 2.5%. Under the same experimental conditions, the conversion from secondary ion intensity to atomic concentration is reproducible from sample to sample within 10–15 %. This enables an accurate evaluation of the relative decrease of the total hydrogen content during annealing, provided that all the H profiles belong to the same set of measurements. We checked the possibility that matrix effects may affect the absolute content assignment, but we found no evidence for this at the quoted accuracy level. Isolated or clustered H_2 molecules that desorb from the sample will evade registration. During the sputtering process, H_2 molecules may be split in two H atoms by the primary beam or, more likely, escape from the surface as a neutral species remaining undetected. Therefore, we cannot exclude that SIMS might have missed (cf. Sec. VI) the H_2 that may form in the bulk upon annealing.

Small-angle x-ray scattering (SAXS). The SAXS system consists of a Kratky compact small-angle system[25] attached to the Rigaku rotating anode (Cu) x-ray generator, a crystal monocromator to select the Cu-K_α radiation, and a proportional counter operated with an Ar-Xe gas mixture. The background count rate with the x-ray shutter closed was as low as about 0.16 counts/s with the detector in the energy window for the 8.05 Cu-K_α x rays. The observed SAXS signals were sometimes only about 2–3 times this rate, so rather long signal averaging was used in collecting the data. A step-scanning mode was used to count the scattered x rays as a function of the momentum transfer $q=(4\pi/\lambda)\sin\theta$ (λ =x-ray wavelength=0.154 nm, 2θ=scattering angle) from about 0.1 to 6 nm^{-1}. The line-collimated x-ray beam was 14 mm$\times$130 μm at the sample and its intensity was measured by the moving slit technique.[25] A typical value of the incident intensity used here was 1.5×10^8 photons/s. Since each scan took about 12–15 h, intensity-drift corrections had to be made by checking the intensity at the start and end of each scan, and assuming linear drift with time (typical intensity changes were quite small -1% to 2%). Scans were repeated 2–3 times and signals averaged. For each SAXS scan a reference scan was made on a crystalline silicon (c-Si) wafer of the same thickness. Since the x-ray absorption by the a-Si(H)+c-Si sample and that by the c-Si reference are identical, a simple subtraction of the reference scan data explicitly yields the additional SAXS from the a-Si(H). The measured difference was normalized by the thickness of the a-Si(H) and the incident intensity, the latter having been corrected for the absorption by the entire thickness of the wafer. The normalized intensity was then converted into electron units [electron/atom (e/a)] using the appropriate geometry factors in the SAXS system and the scattering cross section of the electron ($I_e=7.94\times10^{-26}$ cm^2).[26]

Infrared spectroscopy (IR). Infrared-absorption spectra were measured with a Digilab FTS-40 Fourier-transform infrared spectrometer. The device was equipped with a liquid-nitrogen-cooled $Hg_xCd_{1-x}Te$ detector. To eliminate the effects of multiple reflections of the infrared beam at the interface between amorphous and crystalline Si, spectra were corrected using the procedures of Brodsky, Cardona, and Cuomo[27] and Langford, Fleet, and Mahan.[28]

III. RESULTS

A. Hydrogen profiles—SIMS measurements

Figure 1 shows SIMS profiles measured on both LH and HH samples after implantation and after subsequent annealing at 425, 475, and 525 °C. The as-implanted depth profiles of H exhibit three peaks corresponding to the different implant energies. For the LH sample, the as-implanted H profile peaks at 4 at. %, while the peak is at 20 at. % for the HH sample. A striking difference in the annealing behavior is evident in the two samples. In the case of the low hydrogen concentrations, thermal diffusion at 425 °C yields a complete smearing out of the initially peaked profiles. In contrast, there is no broadening of the H peaks after the anneal at 425 °C in the high-concentration sample. However, H diffusion has occurred since peak intensities decrease in comparison to the as-implanted profile. Furthermore, the concentration level beyond the peaks has increased by one decade, and

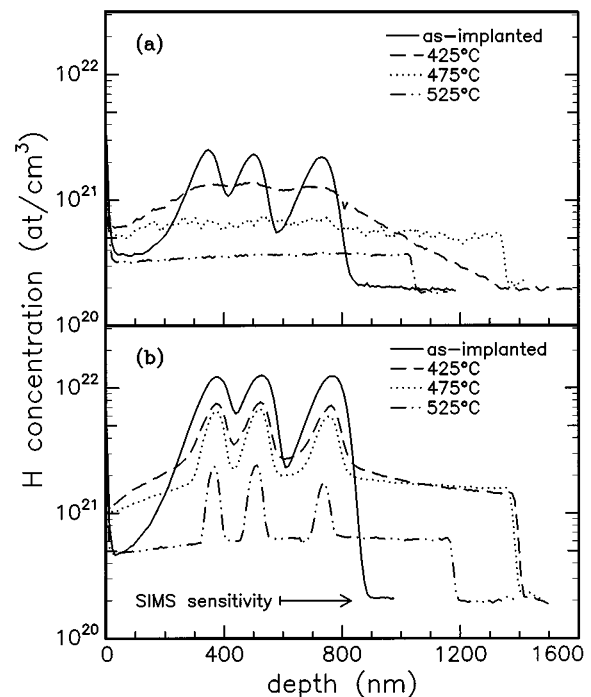

FIG. 1. The hydrogen SIMS profiles for the hydrogenated a-Si samples prepared by ion implantation in the as-implanted state and after annealing of 4 h at 425, 475, and 525 °C. In (a) the low-content (LH) sample, and in (b) the high-content (HH) sample.

has spread out uniformly over the a-Si layer (plateaulike). The H concentration of the plateau in Fig. 1(b) is about 3 at. % after the 425 °C anneal, and it remains at this level after annealing at 475 °C.

With increasing temperature, the differences between annealing behaviors of the two samples become even more pronounced. After the 475 °C anneal, the H distribution of the LH sample becomes uniform throughout the amorphous layer, whereas relatively minor changes in the shape of the depth profile of the HH sample have occurred with respect to the 425 °C annealed state. The distinctive peaks in the HH SIMS profile remain visible even when about 80% of the hydrogen has left the sample after annealing at 525 °C. From integrals of the ion depth distribution, we estimate the retained H doses after annealing, as shown in Table I. The H content has decreased by a factor of 5.5 from the as-implanted to the 525 °C annealed state of the HH sample, whereas this factor is only 2.7 in the case of the LH sample.

The SIMS hydrogen signal of both the LH and HH samples after 425 °C annealing drops abruptly to the sensitivity level (2×10^{20} cm^{-3}) at a depth of ~1400 nm. This position corresponds to the a-Si(H)/c-Si interface. Because

TABLE I. Hydrogen doses (at/cm^2) estimated from SIMS profiles.

Anneal state	LH sample	HH sample
as-implanted	9.4×10^{16}	5.4×10^{17}
425 °C	1.1×10^{17}	4.5×10^{17}
475 °C	7.7×10^{16}	3.7×10^{17}
525 °C	3.5×10^{16}	9.8×10^{16}

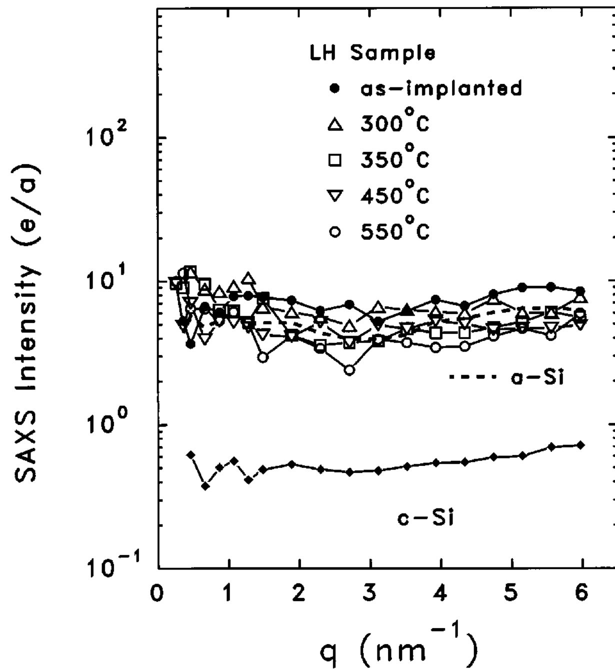

FIG. 2. SAXS intensities from the LH sample in the as-implanted state and after annealing of 4 h at different temperatures. Solid lines are drawn to guide the eye. Also shown are the data from the c-Si reference wafer and from the as-implanted pure a-Si (dashed line) from Ref. 24.

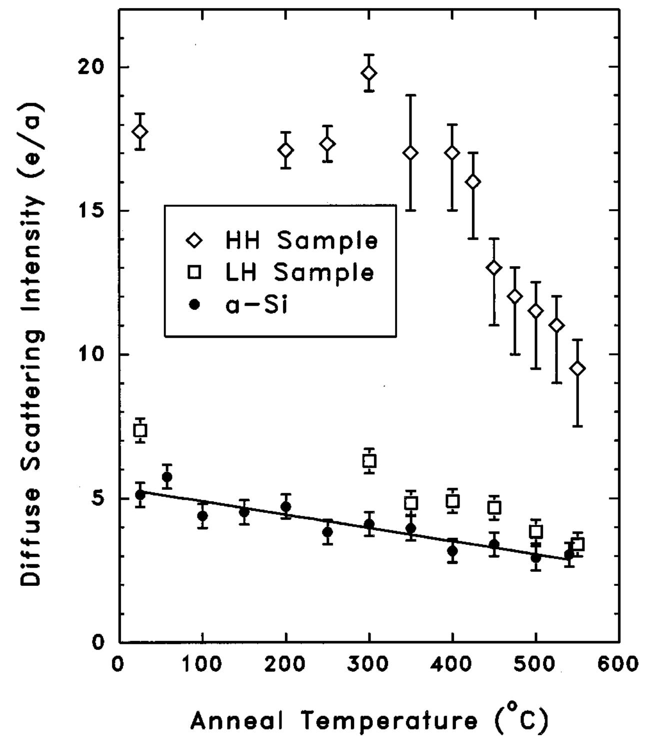

FIG. 3. SAXS diffuse intensity for the hydrogenated a-Si samples LH and HH in the as-implanted state, and after annealing of 4 h from 200 to 550 °C. Also included are the data showing the diffuse scattering for the pure a-Si before and after annealing from Ref. 33.

the solubility of hydrogen is much lower in c-Si than it is in a-Si,[29] hydrogen atoms are prevented from diffusing through the interface into the c-Si bulk.[30] After 525 °C annealing, the drop in H concentration to the background level occurs in both samples at a shallower depth in comparison to the annealing stages at lower temperatures. This indicates that the a-Si(H)/c-Si interface has advanced by solid phase epitaxy (SPE) of ~320 nm in the LH sample and of ~220 nm in the HH sample. For amorphous silicon without H, the recrystallized layer is expected to be larger, i.e., ~720 nm for the presently used 525 °C anneal.[30] Therefore, the SPE rate is slowed by the presence of H. A hindering of growth rate due to H doping has been observed before,[30,31] although in a range of lower H concentrations.[32]

B. Atomic and nanoscale structure—SAXS measurements

LH sample. Figure 2 shows the SAXS intensities from the LH sample compared to those from the unimplanted c-Si wafer, and the a-Si produced by Si implantation prior to H implantation. There is essentially no q dependence in any of the data, which implies that all three samples at all annealing states yield only diffuse SAXS. There is a systematic reduction in the intensity from the LH sample with annealing. If the intensities for a given scan are averaged in the range $1.5 \leq q \leq 6$ nm^{-1}, then the variation shown in Fig. 3 by the open squares results. Included in Fig. 3 are data showing the variation in diffuse intensity with annealing for the pure a-Si, which have been recently presented and interpreted in detail.[24,33] Briefly, the SAXS signal of c-Si is due to thermal diffuse scattering and incoherent Compton scattering, while static-disorder scattering accounts for the increase after amorphization by Si implantation. The good agreement between theoretical calculations of these intensities and the experimental values shows that the nanostructure of the as-implanted and annealed a-Si is homogeneous. In other words, nanovoids are not detected, and if they are present it must be at volume fractions well below 0.1%. A similar conclusion follows regarding the nanostructure of the LH sample, i.e., due to the lack of any q dependence in the SAXS from this sample, there is no evidence of nanovoids or other nanostructural features associated with H clustering, even after anneals up to 550 °C.

The increased diffuse SAXS from the LH sample compared to the pure a-Si shown in Fig. 3 for all annealing temperatures can be attributed in part to the atomic-scale compositional disorder introduced by the H alloying. This effect is known as Laue monotonic scattering,[34] and will be treated more in detail in Sec. IV. Annealing above 300 °C reduces the difference between the LH and a-Si sample diffuse intensities (Fig. 3). This difference reaches zero (within the uncertainty) after the last anneal at 550 °C. This reflects the outdiffusion of H from the a-Si matrix, as observed in Fig. 1(a).

HH sample. Figure 4 shows the SAXS from the as-implanted HH sample, and the dramatic changes caused by the annealing. The as-implanted state displays only diffuse scattering (i.e., no q dependence), but much stronger than that from the LH sample. This is due to the Laue monotonic contribution from the H alloying at higher concentrations. Annealing at 200 and 250 °C caused no change in the SAXS,

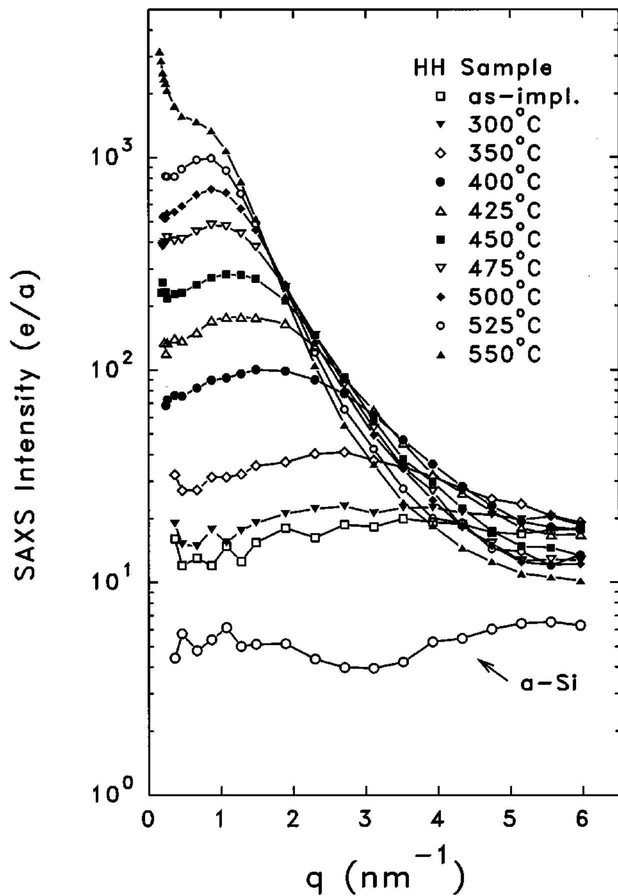

FIG. 4. SAXS intensities from the HH sample in the as-implanted state and after annealing of 4 h at different temperatures. Solid lines are drawn to guide the eye. Also shown are the data from the as-implanted pure a-Si.

and averaging the SAXS intensity over the same range used for the LH sample yields the values of diffuse scattering shown in Fig. 3.

Annealing above 300 °C induces systematic changes in the SAXS corresponding to the formation of low-density nanostructural features of increasing size and volume fraction with temperature. The appearance of a maximum in the intensity is direct evidence of an interference effect due to a high density of scattering centers.[35] The shift of the maximum intensity toward smaller q with increasing temperature indicates an increasing size of inhomogeneities. After the 350 °C anneal their average size is about 0.5 nm, whereas it is 1.55 nm after the last anneal at 550 °C, as a result of the analysis of the data reported in Sec. IV. The systematic drop in intensity at large q is attributed to the loss of H from the matrix which decreases the Laue diffuse scattering. Figure 3 includes the fitted diffuse intensities for the annealing in the temperature range above 300 °C. Values contain a relatively large error because they take only the portion of SAXS at large q, so that evaluation of the diffuse intensity is affected. However, one can clearly see that the data point at 300 °C shows an increased diffuse intensity which then decreases at higher anneal temperatures. After the 550 °C anneal the diffuse intensity has not dropped to the value of the LH or a-Si samples even though much of the H has left the sample according to SIMS (Table I).

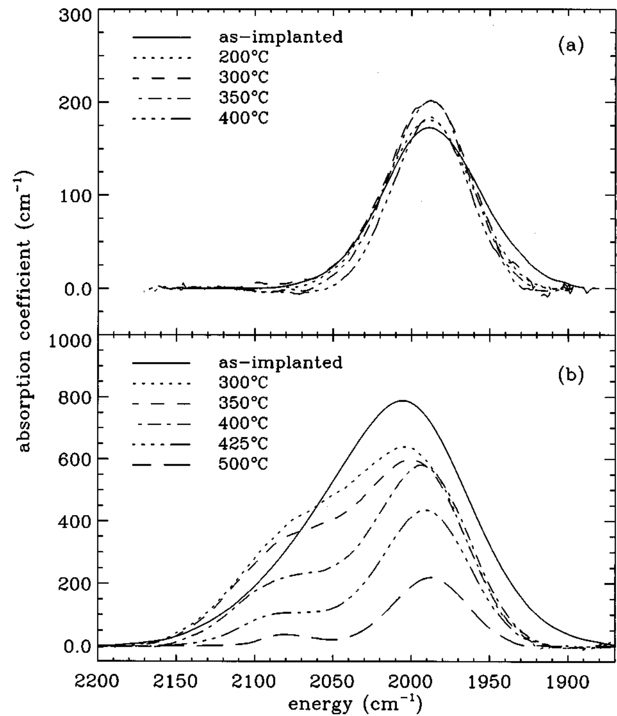

FIG. 5. Infrared-absorption stretching bands of the hydrogenated a-Si in the as-implanted state and after annealing of 4 h at different temperatures. In (a) we show the LH sample, and in (b) the HH sample. Spectra are shown after the background subtraction, using the procedures indicated in Sec. II B.

To test for isotropy in the SAXS, the sample after the 500 °C anneal was also measured in a tilted orientation such that the angle between the surface normal and the x-ray beam direction was 45°. There was no change in the shape or intensity of the SAXS curve, and this is consistent with either spherical scattering objects or randomly oriented nonspheres.

C. Si-H bonds—IR measurements

Infrared-absorption spectra were used to investigate the local bonding configurations of the LH and HH samples before and after annealing cycles. We will focus our attention on two absorption regions of the infrared spectra: the stretching band between 2000 and 2100 cm^{-1}, and the doublet at 800–900 cm^{-1} which results from bending vibrations.[27,36] The features at 2000 cm^{-1} are associated with the stretching modes from isolated Si-H (monohydride) configurations. The modes in the 800–900-cm^{-1} frequency regime are attributed to $Si-H_2$ (dihydride) sites in different local environments, specifically isolated $Si-H_2$ and $(Si-H_2)_n$ (polyhydride) groups.[37] The assignment of the 2070–2100-cm^{-1} modes remains controversial. Although it is widely accepted that these modes (and the 800–900-cm^{-1} modes) originate from dihydride/polyhydride configurations,[37,38] their association with clustered monohydride bonds has also been the subject of a long debate.[39–42]

LH sample. Figure 5(a) shows the stretching bands of the absorption spectra after implantation and annealing of the LH sample. The absorption band of the as-implanted state exhibits only one Gaussian distribution peaked at 2000

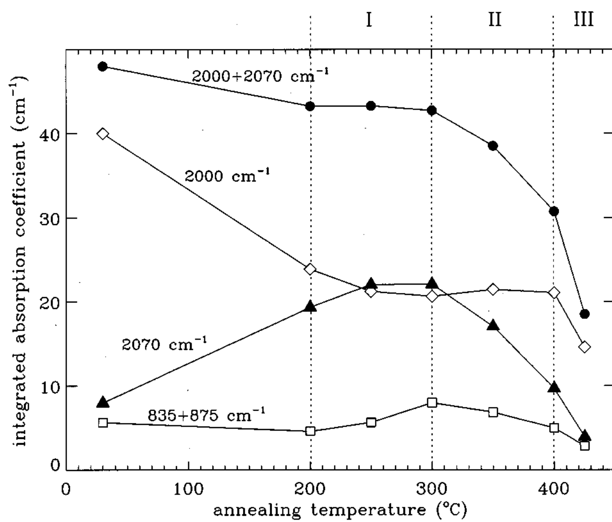

FIG. 6. The integrated absorption coefficient of the 2000-cm^{-1}, 2070-cm^{-1} stretching and bending modes as a function of the annealing temperature for the HH sample. The three regimes of annealing temperatures are indicated by the vertical dotted lines.

cm^{-1}, indicating that the incorporated H is predominantly bonded in the monohydride configuration. Upon annealing, this band remains symmetric while narrowing. Due to the low-H content, the background subtraction and the presence of interference fringes become problematic, so quantitative measurements and reliable integrated intensities cannot be accurately inferred from the spectra.

HH sample. The annealing behavior of the HH sample is more complex than that of the LH sample, as shown in Fig. 5(b) where the stretching-mode absorption bands of the HH sample as a function of the annealing temperature are reported. A broadband peaked at ~2000 cm^{-1} is present in the as-implanted state. After annealing, the absorption band becomes more asymmetric, and the contribution of the modes peaked at 2060–2075 cm^{-1} is more resolved, showing an initial increase up to 300 °C followed by a decrease upon annealing at higher temperatures. This contribution (referred to below as the 2070 modes) is still observable after 500 °C annealing, but after higher-temperature anneals (525–550 °C) the H-related absorption bands can hardly be distinguished from the background (not shown).

The integrated absorption coefficient of the two modes is obtained by fitting the stretching-mode band to two separate Gaussian components. The results are shown in Fig. 6. The total amount of bonded hydrogen can be estimated from the sum of the integrated absorption coefficients of the two modes. A decrease of about 30% in the total intensity is observed during annealing in the range between 300 and 400 °C. Conversely, the total H content, as measured by SIMS, does not change outside of the experimental uncertainty after anneals up to $T=400$ °C. This indicates that the reduced IR absorption is not due to the outdiffusion of hydrogen. The further decrease after annealing at higher temperatures must involve the outdiffusion of hydrogen (see Table I).

The 2070 modes reach a maximum relative value of ~50% of the total absorption signal after the 250–300 °C anneals. The decrease in the regime of 300–400 °C is responsible for the decrease of the total integrated intensity, since the 2000-mode intensity remains flat in this region. In Fig. 6 the integrated intensities of the 800–900-cm^{-1} spectral region are also included. In our spectra a weak doublet peaked at 835 and 875 cm^{-1} is present, and reaches a relative maximum after the 300 °C anneal.

IV. SAXS DATA ANALYSIS

The increase in diffuse scattering intensity of the as-implanted a-Si(H) with respect to pure a-Si is partly due to the H alloying, and is described by the Laue monotonic scattering.[34] This contribution exhibits a particularly simple form for the intensity in electron units in case of a random substitutional $A_{1-x}B_x$ alloy with the same atomic volumes for A and B,

$$I_{\mathrm{LM}}=x(1-x)(Z_A-Z_B)^2, \tag{1a}$$

where Z_A and Z_B are the atomic numbers of the A and B elements. Taking the average H content of the LH sample as $x=0.011$ (from SIMS data), the intensity from Eq. (1a) is 1.7 e/a, in good agreement with the difference in diffuse intensities between the a-Si and LH sample shown in Fig. 3, 2.2±0.6 e/a, for the as-implanted state and up to the 300 °C anneal. Since the atomic volume of H is definitely smaller than that of Si, and the concept of a substitutional alloy may not be appropriate for H in Si (due to the nature of the bonding), this agreement is surprising and might be accidental. A modified expression that accounts for the difference in atomic volume between A and B, $\Omega_A-\Omega_B$, is given by[43]

$$I_{\mathrm{LM}}^{m}=I_{\mathrm{LM}}[1-(\Omega_A-\Omega_B)/\gamma\Omega_A]^2, \tag{1b}$$

where $\gamma=3(1-\nu)/(1+\nu)$, and ν is Poisson's ratio. Using evidence that the atomic volume ratio of H to Si in a-Si:H is near 0.4–0.5,[44,45] and using $\gamma=1.23$ from c-Si, one can estimate that the modified Laue monotonic should be reduced to near 0.4–0.6 e/a, well below the experimental difference noted above. In the case of the HH sample, using the average H content of $x=0.085$ (from SIMS data) in Eq. (1a) and $\Omega_A=\Omega_B$ yields an expected Laue diffuse intensity for a random $\mathrm{Si}_{1-x}\mathrm{H}_x$ alloy of 13 e/a, again in good agreement with the observed increase in diffuse intensity relative to a-Si of 12.8±0.6 e/a (Fig. 3, as-implanted state, and anneals up to 250 °C). Taking into account the difference in atomic volume, Eq. (1b) yields an intensity of 3.4–4.6 e/a, well below the experimental value.

In order to obtain quantitative information on the size and volume fraction of the inhomogeneities as well as values of the diffuse component, the data relative to the HH sample for each anneal temperature were fitted with a theoretical intensity function corresponding to a distribution of spherical objects that are correlated in position by an effective hard-sphere interaction to account for the interference effect:

$$I(q)=C\Sigma_i v_i R_i^2 P(qR_i)S(qD)+I_d, \tag{2a}$$

$$P(qR_i)\equiv P(u)=(9/u^6)(\sin u-u\cos u)^2. \tag{2b}$$

C is a constant fitted to give the intensity in electron units, v_i and R_i are the volume fraction and radius of the ith-sized sphere, $P(qR_i)$ is the form factor for a sphere of radius R_i,[35]

TABLE II. Results of SAXS analyses of the annealed HH sample. T is the anneal temperature (all for 4 h), Q is the integrated intensity [Eq. (3b)], f_1 and f_2 are the total volume fractions of the inhomogeneities based on zero and high-pressure H_2 electron densities, respectively, $\langle R \rangle$ is the volume-fraction-average radius of the inhomogeneities, and D is the effective hard-sphere interaction diameter.

T (°C)	Q (10^{23} e/a cm^3)	f_1 (%)	f_2 (%)	$\langle R \rangle$ (nm)	D (nm)
350	5.2	0.29	0.40	0.50	1.9
400	11.5	0.65	0.89	0.72	2.5
425	16.1	0.91	1.26	0.81	3.2
450	21.0	1.20	1.65	0.96	3.5
475	27.2	1.55	2.14	1.08	4.1
500	31.9	1.83	2.53	1.25	4.6
525	36.1	2.08	2.87	1.39	5.3
550	42.9	2.47	3.47	1.55	5.7

$S(qD)$ is a pair correlation structure factor for hard spheres of diameter D,[46] and I_d is a constant to account for the diffuse scattering. Equation (2) is appropriate to line-focus conditions.[47] The value of D is closely related to the location of the maximum in $I(q)$.[48] To fit the data in Fig. 4, it was necessary to include only 1–3 different sphere radii, and the fits are essentially indistinguishable from the solid lines that connect the points shown in the figure. For fitting the 550 °C data, a third term was added, namely a Porod term,[35] $\sim q^{-3}$, to Eq. (2) to account for the rise in intensity at the lowest q caused from some larger-sized objects which appear on the surface as a result of this last anneal. The total volume fraction of inhomogeneities, f, was determined from the expression appropriate to a two-phase system studied with a line-focus SAXS system:[26]

$$f(1-f)=Q/2\pi^2\langle\Omega\rangle(\Delta n)^2, \tag{3a}$$

$$Q=(q_s/2)\int q[I(q)-I_d]dq, \tag{3b}$$

where q_s is a constant determined by the SAXS slit geometry, $\langle\Omega\rangle$ is the average atomic volume of the sample, and Δn is the electron-density difference between the hydrogenated matrix and the low-density features. We have calculated values of f from the experimental data in Fig. 4 assuming two values of the electron density in the inhomogeneities, zero (i.e., assuming they are voids) and 9.7×10^{22} cm^{-3}. The latter value is that associated with a hydrogen pressure of 0.2 GPa in the inhomogeneities, for which there is experimental evidence in the case of H_2 molecule clusters in a-Si.[49] The electron density of the matrix was taken as 5% lower than that of c-Si to account approximately for the H alloying and the intrinsic density deficit of 1.8% for a-Si.[22]

Table II lists the results of the analyses of the SAXS data via Eqs. (2) and (3), including the average radius of the inhomogeneities $\langle R \rangle=\Sigma_i v_i R_i$, D, and f. The volume fraction increases to 2.5–3.5 % at the highest anneal temperature. Further anneals at 550 °C up to 20 h produced a further small increase in Q (to 44.2×10^{23} e/a cm^3 after 8 h) and then a decrease (to 36.3×10^{23} e/a cm^3 after 20 h) probably due to recrystallization of a-Si by SPE. The average inhomogeneity size and the hard-sphere diameter increase systematically with the anneal temperature in Table II, and a plot reveals linear increases of both within experimental error (i.e., ±0.1 nm for $\langle R \rangle$ and ±0.2 nm for D). Both extrapolate to zero at $T=264$ °C suggesting this as the initial formation temperature of the inhomogeneities.

V. DISCUSSION

A. Pure amorphous silicon

The maximum volumetric fraction of nanovoids in ion-implanted pure a-Si is well below 0.1%, and no void nucleation occurs during thermal treatments, i.e., during structural relaxation.[24] By contrast, pure a-Si films prepared by deposition always exhibit nanovoids, suggesting that voids are an artifact of the preparation method. The absence of nanovoids in ion-implanted a-Si invalidates the statement, originating from molecular-dynamics simulations,[4] that a structure containing voids (of a size corresponding to several missing Si atoms) is energetically favorable since voids would decrease the local strain of the network, at least for pure a-Si. Therefore, the 1.8% deficit of the atomic density observed in ion-implanted a-Si with respect to c-Si (Ref. 22) is not due to voids. Possible causes for the density deficit are (1) a lengthening of the Si-Si bonds, or (2) an imbalance of density change due to vacancy/interstitial-type defects.[24]

Deposited a-Si:H films generally contain inhomogeneities, and the question of whether the hydrogen plays a role in their formation has not been answered unambiguously. In the remainder of this section, we will demonstrate that inhomogeneity formation is *not only* an artifact of the deposition method, but that hydrogen may cause it. More importantly, the drastically different behavior of the LH and HH samples confirms that the H concentration is a critical parameter in the structural quality and stability of the material. In this section we discuss the results presented in Sec. III, separating the as-implanted state from the evolved structure. The evolution of the structure of the HH sample will be divided into three regimes of annealing temperatures: (I) $T\leqslant300$ °C, (II) 300 °C$<T\leqslant400$ °C, and (III) $T>400$ °C.

B. As-implanted state of hydrogenated amorphous silicon

The hydrogenated layers are characterized by a nonuniform H distribution with maximum concentration at the implantation peaks of 4 at. % in the case of the LH sample and 20 at. % in the HH sample, as measured by SIMS (Fig. 1). In the as-implanted state, almost all the H is expected to be bonded to Si after implantation with monohydride bonds as the preferred configuration in a-Si hydrogenated by ion implantation.[45,50] This preferential bonding has been explained as an effect of irradiation, ion bombardment causing the transfer from dihydride to monohydride centers. This conversion from dihydride to monohydride has been found to occur only for [H]$\leqslant$3 at. %.[50]

The IR spectrum of the as-implanted state of the LH sample shows no 2070 modes [Fig. 5(a)], indicating that all the H is bonded as Si-H configurations, in agreement with previous investigations. In the as-implanted HH sample, the

absorption band is slightly asymmetric and the intensity of the 2070 modes is of the same order as that of the bending modes (Fig. 6), i.e., ~16% of the total integrated intensity of the stretching modes. This suggests the presence of polyhydride centers. The x-ray intensities of both the LH and HH samples show no evidence of a q dependence in the as-implanted state. This indicates that ion bombardment does not induce nanoscale inhomogeneities at the fluences under study, i.e., up to 20 at. %, and that the samples are stable against H-induced void formation during implantation at liquid-nitrogen temperature or after irradiation at room temperature.

In Fig. 3, a difference in diffuse scattering intensity is evident between the as-implanted state of the LH, HH, and pure a-Si samples. This difference can be attributed to a difference in static disorder,[33] and to the presence of H atoms which act as scattering centers. A random distribution of H atoms leads to atomic-scale composition fluctuations which are described by the Laue monotonic scattering given by the expressions in Eq. (1). The values for I_{LM} obtained using Eq. (1a) fully compensate for the difference of the experimental diffuse intensity illustrated in Fig. 3 between pure and hydrogenated a-Si for both samples. Therefore, assuming that the atomic volumes of H and Si are the same, this would indicate that the static disorder of the Si network structure, as measured by SAXS, is the same in the as-implanted state of the LH, HH, and pure a-Si samples. This result would not be surprising because the defective state of the as-implanted samples before and after the hydrogenation at *both* fluences is expected to contain the same amount of disorder, since all samples were implanted up to the maximum damage level.[21]

Although this simple interpretation of the results is tempting, the volume difference between H and Si has to be considered, and Eq. (1b) gives values of I_{LM} much smaller than the experimental ones. A possible explanation for this difference is the presence of vacancy-type defects, correlated with the presence of H,[51,52] which would increase the Laue contribution according to Ref. 43, $I_{\mathrm{LM}} \approx NcZ^2$, where c is the atomic fraction of vacancies clustered as N vacancies per cluster ($N=1$, a monovacancy), and Z the atomic number of Si. In other words, the apparent enlarged volume for H could be due to those H atoms associated with a vacancy (or divacancy) in the network structure. For the high-concentration sample, the scattering intensity may be enhanced by the presence of the small amount of polyhydride centers (see IR spectra); i.e., as in the above expression, dihydrides would contribute more effectively than monohydrides.

Since several experiments have detected the presence of trapped H_2 molecules in as-deposited a-Si:H at levels from 0.05 to 0.5 at. %,[53–56] the H_2 molecule should also be considered as a possible configuration of H in the as-implanted state of our samples. In the case of implanted material, it has been suggested[45] that nuclear collisions induce H_2 formation by activating two neighboring Si-H bonds or a Si-H_2 bond. Only two H atoms which are near neighbors are capable of forming H_2, since their deexcitation time is very short ($<10^{-10}$ s). Thus the H_2 formation as a result of ion bombardment likely occurs only in the HH sample, and not in the LH sample. However, the amount of H in H_2 molecules appears to be relatively small in the present experiments, since the total amount of bonded hydrogen estimated from the IR-absorption coefficient[39] agrees with the incorporated H dose (Table I) to within 10%.

C. Low-concentration (LH) sample

The SAXS data presented in Fig. 2 show no q dependence in the scattering intensity of the LH sample after annealing cycles through 550 °C. We therefore conclude that the volume concentration of the nanoscale inhomogeneities (voids or H-rich clusters) can be at most 0.1%. Information on the structural evolution on a scale smaller than 1 nm can be deduced from the study of the diffuse scattering intensity (Fig. 3). The diffuse intensity systematically decreases with increasing annealing temperature similar to pure a-Si. The decrease in scattering of pure a-Si has been interpreted as a decrease in static disorder during structural relaxation.[33] The similar behavior exhibited by the LH sample indicates that the silicon network relaxation is neither perturbed nor enhanced by the presence of 3–4-at. % hydrogen, consistent with previous results,[57] obtained by studying the bond angle distortion from Raman-scattering spectra.

The stretching band of the IR spectra narrows during annealing, suggesting a reduction in the energy distribution of the Si-H bonds which could arise from structural relaxation in the underlying a-Si network. Local ordering during annealing at $T \leqslant 300$ °C induces H atoms to settle into more stable configurations (deep trapping states), and all the H is expected to remain bonded as monohydride. At temperatures higher than 300 °C, H can be released from the bonds to the transport level leading to diffusion.[58,59]

SIMS measurements in Fig. 1(a) show that the three-peaked as-implanted Gaussian-shaped H profile has evolved into a flat-topped depth distribution after 425 °C annealing. We estimate the *effective* diffusion length L_{eff} by comparing three Gaussian fits to the measured profiles before and after diffusion. The value obtained for L_{eff} is ~0.5 μm for the 475 °C profile, five times lower than that found in undoped a-Si:H,[60,61] for which results could be described by a single activation energy of 1.5 eV for the diffusion process. Unfortunately, the little data available in the literature on ion-implanted hydrogenated a-Si appear not to be in agreement on the diffusion coefficient,[62–64] making the comparison with the present result difficult. However, these results clearly show that L_{eff} and diffusivity are dependent on H and defect concentrations.

D. High-concentration (HH) sample

1. Regime I ($T \leqslant 300$ °C)

Upon annealing at $T \leqslant 300$ °C, again no q dependence is evident in the SAXS scattering intensity of the HH sample. Thus the annealing within this temperature range does not lead to the formation of low-density nanofeatures. The diffuse intensity does not change up to 250 °C within the experimental error, while it increases after the 300 °C anneal. This rise in intensity is likely associated with an increase of Si-H_2/(Si-H_2)$_n$ units and/or of small clusters of Si-H which

would increase the Laue monotonic contribution if the number of such clusters becomes larger than expected for a random alloy.[34]

IR results are also consistent with a partial transfer upon annealing from monohydride to polyhydride bonding configurations. After the first annealing at 200 °C, the 2000 and 2070 modes exchange intensity and they become of the same order after the 250 and 300 °C anneals. The relatively strong increase in the 2070 modes is accompanied only by a slight increase of the bending modes, as is evident from the weak absorption bands present in the 800–900-cm^{-1} region. However, the ratio between the 2070-cm^{-1} intensity and bending absorption strength has been seen to depend on sample preparation,[42] suggesting that the weakness of the bending modes could be characteristic of ion-implanted material. We therefore associate the presence of the bending modes together with that of 2070 modes with Si-H_2/(Si-H_2)$_n$ bonding configurations. In other words, IR results suggest an increase of polyhydride centers during annealing at $T \leqslant 300$ °C, in agreement with the interpretation given from SAXS results.

During annealing at $T \leqslant 300$ °C, a rearrangement of H atoms in the matrix is thought to occur via local bond switching[65] with eventual passivation by H of dangling bonds. In this regime, the release of H from deep defect states is improbable, and only the H atoms which after implantation are situated in shallow traps (e.g., in interstices) have the possibility to rearrange locally because of their low binding energy (0.2–0.5 eV).[58,59,66] Thus the possible processes occurring at this stage are an accommodation of near-neighbor Si-H bonds via bond switching and a release of H from disorder-induced shallow states. These processes presumably take place *without* H_2 formation because of the low temperatures involved. Since only near-neighboring H atoms can interact with each other in this regime of temperatures, changes in the configurational distribution towards an increase of H bonded in polyhydride centers occur only in the high-concentration sample. As discussed in Sec. V C, in the low-concentration sample local ordering arranges the H atoms into deeper states. As a consequence of the local scale of the reordering, the SAXS intensity cannot reveal changes in the nanostructure, and therefore no q dependence appears in the scattering signals during anneals in this regime. Furthermore, SIMS measurements on H implanted a-Si have shown no difference in the H distribution profiles between the as-implanted state and the samples annealed at 300 °C,[67] confirming that no long-range diffusion occurs.

2. Regime II (300 °C<$T \leqslant$400 °C)

After the 350 °C anneal, the scattering signal of the HH sample shows a clear q dependence. This indicates the presence of low-density features with sizes of about 0.5 nm and a content of 0.35 ± 0.05 vol. %, as determined by fitting the SAXS intensity (Table II). The increase of the x-ray signal after the 350 °C anneal is accompanied by a drop in the diffuse intensity which continues to decrease at higher anneal temperatures. This drop may indicate a loss of hydrogen from the matrix, with a consequent reduction of the atomic-scale scattering centers and therefore of the Laue monotonic contribution [Eq. (1)]. Another possible explanation is the reduction of polyhydride centers (those smaller than ~0.5 nm and then not visible by SAXS as a q dependence) during annealing. Since the decrease of the diffuse scattering intensity coincides with a systematic increase in content and size of the inhomogeneities, we suggest that the H which leaves the matrix undergoes clustering into nanofeatures.

This picture is confirmed from study of the evolution of the IR spectra upon annealing. The total integrated absorption coefficient of the stretching bands decreases by about 30% as a result of the anneals between 300 and 400 °C. Since the total integrated intensity is proportional to the H content,[39,68] we conclude that the amount of bonded H diminishes during annealing. On the other hand, the *total* H content at $T \leqslant 400$ °C, as measured by SIMS, does not change within the resolution. This suggests that at this temperature regime H leaves the bonds while remaining inside the sample. It also appears that SIMS is able to detect the entire H population, at least in this temperature regime. Figure 6 illustrates that the decrease in the total strength of the stretching band is entirely caused by a reduction of the 2070 modes. The value of the intensity associated with the 2070 band after the 400 °C anneal is as small as that of the as-implanted state. This decrease is accompanied by a decrease of the weak intensity of the bending modes, indicating that H leaves the bonds preferentially from the (Si-H_2)$_n$ (with $n \geqslant 1$) groups. If we assume that polyhydride centers constitute at least part of the clustered phase of H in a-Si,[69,70] the preferential release of H from the polyhydride groups seen in our data is in agreement with a model recently proposed,[71,72] that the H in the clustered phase is situated in a shallower trap (~1.4 eV) than the H in the isolated phase (~2.1 eV).

The decrease of the 2070 modes at temperatures higher than 300–350 °C has been generally observed in deposited a-Si:H films by several authors.[39,73] The systematic decrease of the 2070-cm^{-1} band has been interpreted[74] by assuming that two neighboring Si-H bonds (or a Si-H_2 bond) break with simultaneous formation of a H_2 molecule which may escape from the sample. It is generally accepted that at temperatures around 300–350 °C two neighboring H atoms recombine with H_2 formation,[58,65] a process characterized by an effective activation energy of 1.7 eV.[74]

The process of H_2 formation during annealing at $T > 300$ °C in the high-concentration sample may also occur in the reverse direction; i.e., the formed molecules dissociate again with simultaneous creation of two Si-H bonds. However, the H_2 molecule configuration probably remains stable if it is trapped in a H cluster which becomes enriched by H_2 and enlarges in size, as seen from the increase of the SAXS scattering signal. Since H primarily leaves the clustered phase, we can assume the existence of a critical size for the H clusters. Those smaller than the critical size shrink, by forming H_2 molecules, while the larger ones grow by attracting H atoms from the local surrounding. The coarsening of bubbles resembles the kinetics of metal precipitation generally observed in Si.[75] Thermal-induced coarsening leads to the growth of large precipitates at the expense of the small ones, a phenomenon known as Ostwald ripening. Therefore, we conclude that the inhomogeneities visible by SAXS in the HH sample are H_2 bubbles formed from the precipitation of the hydrogen which cannot be dissolved as stable Si-H bonds in the a-Si matrix. The formation of bubbles in hydrogenated a-Si appears to be a direct consequence of the fact that there

is an intrinsic limit to the solubility of H in *a*-Si.

Previous experiments have established that the H_2 contained in *a*-Si:H-deposited films is in the form of clusters with a lower size limit of ten H_2.[76] These results have been confirmed by IR measurements[49] which demonstrate that H_2 is incorporated in *a*-Si:H in the form of high-pressure bubbles. Thus the volume fraction of the bubbles in this temperature regime is reasonably given by f_2 (Table II), i.e., values which were estimated by assuming a bubble pressure of 0.2 GPa as shown from the good agreement between Eqs. (A1) and (A2) of the Appendix.

Table II reports the bubble radius $\langle R \rangle$, while D represents the size of the region around each bubble from which the H is diffused to form the bubble. It is therefore quite reasonable that D is significantly larger than $\langle 2R \rangle$, since D is expected to represent the size of the H diffusion zone around the average precipitate of H_2. That is, D is the diameter of the depletion sphere that acts like a hard-sphere pair-correlation interaction that is larger than the precipitate itself.[48] However, the values for f listed in Table II are much smaller than volume fractions expected to yield such strong interparticle interference effects.[35,48] This can be readily attributed to the nonuniform distribution of H (Fig. 1), so that the precipitation of the H occurs only in some fraction of the layer corresponding to the peaks in the profile where the local H solubility is exceeded. The nonuniform H distribution is a peculiarity of ion-implanted *a*-Si(H), and marks the difference from deposited *a*-Si:H films. Cross-sectional transmission electron micrographs on the 550 °C-annealed sample[77] show bubble bands in the fractions of the layer corresponding to the H-peak concentrations, with bubble sizes increasing with H concentration toward the peaks of the H distribution. Therefore the local volume fraction of the bubbles is much higher than the values of f in Table II, since these values are averages over the entire layer thickness.

3. Regime III ($T>400$ °C)

The SAXS signal increases with annealing at $T>400$ °C, indicating that the accumulation of hydrogen in bubbles as H_2 molecule formation continues. H_2 molecules trapped in voids in *a*-Si:H are thought to be stable until fairly high temperatures ($\sim$500 °C).[78] It is noteworthy that the 4-h anneal at 550 °C caused a significant change in the HH sample. Optical microscope examination revealed that about 30% of the hydrogenated layer had delaminated from the *c*-Si substrate in the shape of circular regions about 20 to 100 μm in diameter (this loss of material was corrected for in the Q calculation at 550 °C). Since all the holes appear to have the same depth, the phenomenon likely takes place originally at the *a*-Si(H)/*c*-Si interface, which moves by SPE toward the surface. Hydrogen diffusion induces an accumulation of H_2 molecules in high-pressure bubbles at the interface. The rising pressure eventually opens the bubbles via explosion, with consequent delamination of the hydrogenated layer visible in large regions of the surface. Similar blistering of the surface was observed in deposited *a*-Si:H films[39,79] where holes were also associated with an accumulation of gaseous H at the film/substrate interface. No further delamination occurred upon longer time annealing at 550 °C. Several pieces of the delaminated material were collected, and a flotation density measurement was made. A value of 2.24 ± 0.02 g/cm^3 was obtained. Allowing for an intrinsic deficit of 1.8%,[22] shown not to be due to nanovoids,[24] the remaining deficit is 2.1 $\pm$0.8% which is in good agreement with the value for f_1 in Table II. We actually expect a better agreement with f_1 than f_2 since most of the H has left the sample at this stage of annealing (Table I) such that the larger electron density contrast in the f_1 calculation is more appropriate.

VI. SOLUBILITY AND DIFFUSIVITY OF HYDROGEN; CLUSTERING PROCESS

The diffusion behavior observed in the H profiles of the high-concentration sample differs entirely from that of the low-concentration sample (Fig. 1). In this case, peaks of the implanted profiles do not broaden after annealing while decreasing in height. The diffusion profiles clearly show that hydrogen does not penetrate the nonhydrogenated amorphous material below the peaks and the low-concentration regions between the peaks for concentrations exceeding 3 at. %. Apparently, the spreading of the profiles of the HH sample into the nonhydrogenated regions is prevented because H atoms cannot find available sites. In other words, the material is impermeable to hydrogen for concentrations higher than $\sim 1.5\times10^{21}$ cm^{-3}. This result is consistent with the observation that the hydrogen in the LH sample shows regular diffusion over the entire concentration range, i.e., $\leqslant$4 at. %. Thus the difference in the annealing behavior of the two samples can be explained in terms of solubility of H in the matrix. The diffusion profiles in the HH sample indicate a demarcation between soluble and nonsoluble hydrogen. The solubility of hydrogen in *a*-Si at 425–475 °C is limited to 3–4 at. %.

The data in Fig. 1 suggest that the diffusivity into the nonhydrogenated region (900–1400 nm) is larger in the HH sample than in the LH sample. Thus the diffusion process is concentration dependent. As a consequence of the higher diffusivity, the flux to the surface is higher in the HH than in the LH sample. This observation is confirmed by the fact that the retained dose in the HH sample after the anneals up to 525 °C is a factor of 2 smaller than the one retained in the LH sample (see Table II). At this point, the possibility that the H content measured by SIMS does not include the H present in the bulk as H_2 molecules (as discussed in Sec. II B) has to be considered. Although this likely underestimates the values of the doses in the annealed HH sample, it may not completely account for the factor of 2 difference in the reduction of the H doses between the HH and LH samples. The enhancement of diffusivity with H concentration can be considered to be in agreement with a recent study[72] where two distinct rate processes were observed in the decrease of the bonded H content during annealing of *a*-Si:H films, the faster process associated with the H in the clustered phase.

The defect concentration present in as-implanted *a*-Si has been found to lie between 1 and 2 at. %; thermal treatments induce network rearrangements while reducing the density of defects.[20,21] Structural defects in *a*-Si have also been probed using fast-diffusing impurities (such as Cu, Au, and Pd), the defects acting as trapping centers for these impurities.[80,81] It was shown that the diffusion and solubility of the impurities

are intimately related to the defect state of *a*-Si. The reduction of the defect density during structural relaxation of *a*-Si decreases the solubility of these fast diffusers while increasing their diffusion coefficient. In a similar study,[64] it was suggested that the defects also serve as traps for H atoms, with H more strongly bonded than the metal impurities. The trap density measured in those experiments was 2.2±0.9 at. % for 350 °C annealing. If in our case we also assume a direct correlation between trap density and H solubility, we conclude that the trap density is 3–4 at. % in the 425–475 °C temperature range. This value is in good agreement with that found in Ref. 64, though it has been measured at a higher temperature, where a smaller number of trap centers would be in principle expected due to further defect annihilation. The concept of the presence of a limited concentration of trap centers for H in the *a*-Si matrix is also an important insight for the *a*-Si:H technology, and raises a serious question about the models in which an unlimited number of traps for H was assumed in Si.[59,82,83]

By investigating ion-implanted *a*-Si, we have shed light on the relative roles of the hydrogen and the *a*-Si network, providing clear evidence of the presence of a well-defined limit in the defect-related trap concentration in the *a*-Si matrix. Amorphous silicon has a highly defective structure containing a variety of defects,[21,84] e.g., point defects, and strained Si-Si bonds, of which only a small amount consists of paramagnetic defects (i.e., dangling bonds).[85] The addition of H to this network leads to a passivation of most of the defects, with a possible relief of the local strain. During annealing, the hydrogenated *a*-Si undergoes structural relaxation, exhibiting a decrease in static disorder similar to pure *a*-Si. Therefore, results would indicate that defect passivation by means of H is an independent mechanism from structural relaxation, as was suggested in Ref. 20 and very recently shown in Ref. 86. Results furthermore demonstrate that hydrogenated *a*-Si does not necessarily evolve upon annealing into an inhomogeneous structure containing nanovoids, or other H-related clusters, as long as H can be dissolved as a stable monohydride.

However, the addition of H into *a*-Si at a concentration exceeding that of defects produces an unstable structure. In this case, H atoms in excess have to settle into unstable nondefect configurations, thus building the local strain in the network. During annealing, the strain associated with the H in unstable sites can be released only by the precipitation of the excess H through its clustering. The evolution of H clustering resembles the precipitation of dopants and metals in Si through Ostwald ripening,[75] which also occurs when the impurity concentration exceeds the solubility. It is worthwhile to note that H_2 bubbles, thought to originate from H_2 supermolecular configurations,[87] are generally observed in H-implanted *c*-Si after annealing,[88,89] although at lower H concentrations because of the much lower H solubility in *c*-Si compared to *a*-Si.

VII. SUMMARY AND CONCLUDING REMARKS

In this paper, we have presented systematic studies of hydrogen implanted into pure amorphous silicon (*a*-Si) layers using SAXS, SIMS, and IR techniques. This investigation shows that the H concentration determines the atomic and nanoscale structures of the hydrogenated *a*-Si during subsequent annealing regimes. Hydrogen atoms can be accommodated in the *a*-Si matrix only at concentrations up to 3–4 at. %, which is found to be the solubility limit of H in *a*-Si in the 425–475 °C temperature range. For alloys containing H below this solubility limit, the network structure is stable, and remains homogeneous during annealing. Conversely, if H is introduced into the matrix with a concentration well above this solubility limit, the alloy is not stable, and the excess H tends to leave the matrix at relatively low temperatures (>300 °C) to form H_2 molecules. In this regime, a low density of nanoscale inhomogeneities appears, increasing systematically in size during further anneals. These inhomogeneities are thought to be H-rich clusters where H_2 molecules are trapped, i.e., H_2 nanobubbles. The passage from homogeneous structure to one containing nanobubbles of about 0.5 nm of radius must be gradual, and it is possible that the disklike H platelets (containing 6–10 H atoms) thought to result from clustering of the diatomic H_2^* complexes,[86] and observed by nuclear magnetic resonance,[69,70] are the precursors of the larger features observed at $T>300$ °C by SAXS.

Finally, we want to emphasize that it is always possible to introduce H in amorphous silicon well above the solubility limit by various nonequilibrium methods with no detectable inhomogeneities in the original structure. However, upon thermal treatments H atoms can be stably bonded only to the network sites set by the defect concentration inherent to the network. These defect-related trapping sites define the solubility of H in *a*-Si. All the trapping sites being saturated, the excess H clusters during annealing and forms H_2 molecules which gather into nanobubbles.

ACKNOWLEDGMENTS

The authors express sincere thanks to J. S. Custer for his suggestions in the early stage of the work, and to A. Polman for many useful discussions. We also wish to acknowledge W. G. J. H. M. van Sark for his help in preliminary measurements and interpretations, J. Daey Ouwens for sharing his knowledge on IR spectra analysis, and T. Weber for technical help. We are indebted to W. Beyer for informative discussions on H diffusivity in differently prepared amorphous silicon samples, and for the effusion measurements on the as-implanted SIMS samples. This work is part of the research program of the Foundation for Fundamental Research on Matter (FOM), and was made possible by financial support from the Netherlands Organization for Scientific Research (NWO). The work at Colorado School of Mines was supported by the National Renewable Energy Laboratory (NREL) under Contract No. XAN-4-13318-04. One of us (S.A.) acknowledges the support of the Università di Padova.

APPENDIX: CONSISTENCY CHECK OF THE H_2 -BUBBLE PRESSURE

We estimate the number of H_2 molecules trapped in the bubbles in the HH sample annealed at 400 °C. The number

of H_2 molecules per unit volume, N_{H_2}/V_{H_2}, is given by the ideal gas equation

$$\frac{N_{H_2}}{V_{H_2}}=\frac{p}{kT}=4.8\times10^{28}\ \mathrm{m}^{-3}, \qquad \text{(A1)}$$

where p is the bubble pressure at room temperature, i.e., 0.2 GPa,[49] k is Boltzmann's constant, and T=300 K. From IR results, the H loss upon annealing between 300 and 400 °C is about 30%, which is equivalent to 2.55 at. %, assuming 8.5 at. % as the average H concentration (from SIMS). Taking f_2=0.9 vol.% from Table II, Eq. (A1) can be written as

$$\frac{N_{H_2}}{V_{H_2}}=\frac{(0.0255/2)N_{\mathrm{Si}}}{0.009V_{\mathrm{Si}}}\approx1.4\ \frac{N_{\mathrm{Si}}}{V_{\mathrm{si}}}=6.6\times10^{28}\ \mathrm{m}^{-3}, \qquad \text{(A2)}$$

where $N_{\mathrm{Si}}/V_{\mathrm{Si}}$ is the density of the hydrogenated a-Si matrix, taken to be 5% lower than c-Si.

The values calculated from Eqs. (A1) and (A2) are in agreement within the experimental uncertainty, indicating a consistency between the number of H_2 molecules in the bubbles and the pressure inside them. The agreement would be exact if we assume a pressure of 0.27 GPa.

---

*Permanent address: Energieonderzoek Centrum Nederland (ECN), P.O. Box 1, 1755 ZG Petten, The Netherlands.

[1] For a recent review, see, e.g., R. A. Street, *Hydrogenated Amorphous Silicon* (Cambridge University Press, Cambridge, 1991), p. 18.

[2] A. H. Mahan, Y. Chen, D. L. Williamson, and G. D. Mooney, J. Non-Cryst. Solids **137&138**, 65 (1991).

[3] R. Bellissent, in *Amorphous Silicon and Related Materials*, edited by H. Fritzsche (World Scientific, Singapore, 1988), p. 93.

[4] R. Biswas, I. Kwon, A. M. Bouchard, C. M. Soukoulis, and G. S. Grest, Phys. Rev. B **39**, 5101 (1989).

[5] A. H. Mahan, D. L. Williamson, B. P. Nelson, and R. S. Crandall, Solar Cells **27**, 465 (1989).

[6] P. D'Antonio and J. H. Konnert, in *Tetrahedrally Bonded Amorphous Semiconductors*, edited by R. A. Street, D. K. Biegelson, and J. C. Knight, AIP Conf. Proc. No. 73 (AIP, New York, 1981), p. 117.

[7] A. J. Leadbetter, A. A. M. Rashid, N. Colenutt, A. F. Wright, and J. C. Knight, Solid State Commun. **38**, 957 (1981).

[8] S. Guha, J. Yang, S. J. Jones, Y. Chen, and D. L. Williamson, Appl. Phys. Lett. **61**, 1444 (1992).

[9] S. J. Jones, Y. Chen, D. L. Williamson, U. Kroll, and P. Roca i Cabarrocas, J. Non-Cryst. Solids **164–166**, 131 (1993).

[10] D. L. Williamson, in *Amorphous Silicon Technology–1995*, edited by M. Hack, E. A. Shiff, A. Madam, M. Powell, and A. Matsuda, MRS Symposia Proceedings No. 377 (Materials Research Society, Pittsburgh, 1995), p. 251.

[11] J. Shinar, H. Jia, R. Shinar, Y. Chen, and D. L. Williamson, Phys. Rev. B **50**, 7358 (1994).

[12] M. J. van den Boogaard, S. J. Jones, Y. Chen, D. L. Williamson, R. A. Hakvoort, A. van Veen, A. C. van der Steege, W. M. Arnold Bik, W. G. J. H. M. van Sark, and W. F. van der Weg, in *Amorphous Silicon Technology—1992*, edited by M. J. Thompson, Y. Hamakawa, P. G. LeComber, A. Madan, and E. A. Schiff, MRS Symposia Proceedings No. 258 (Materials Research Society, Pittsburgh, 1992), p. 407.

[13] E. S. Machlin, *Materials Science in Microelectronics, The Relationship Between Thin Film Processing and Structure* (Giro, Croton-on-Hudson, 1995).

[14] C. Manfredotti, F. Fizzotti, M. Boero, P. Pastorino, E. Vittone, and V. Rigato, Phys. Rev. B **50**, 18 046 (1994).

[15] Y. Chen, S. J. Jones, D. L. Williamson, S. Yang, N. Maley, and J. R. Abelson, in *Amorphous Silicon Technology—1992* (Ref. 12), p. 311.

[16] A. H. Mahan, B. P. Nelson, S. Salomon, and R. S. Crandall, in *Amorphous Silicon Technology—1991*, edited by A. Madan, Y. Hamakawa, M. Thompson, P. C. Taylor, and P. G. Lecomber, MRS Symposia Proceedings No. 219 (Materials Research Society, Pittsburgh, 1991), p. 673.

[17] P. Papadopulos, A. Scholz, S. Bauer, B. Schröder, and H. Oechsner, J. Non-Cryst. Solids **164-166**, 87 (1993).

[18] R. Zedlitz, F. Kessler, and M. Heintze, J. Non-Cryst. Solids **164-166**, 83 (1993).

[19] J. M. Poate, in *Amorphous Silicon and Related Materials*, edited by H. Fritzsche (World Scientific, Singapore, 1989), p. 149.

[20] S. Roorda, W. C. Sinke, J. M. Poate, D. C. Jacobson, S. Dierker, B. S. Dennis, D. J. Eaglesham, F. Spaepen, and P. Fuoss, Phys. Rev. B **44**, 3702 (1991).

[21] P. A. Stolk, F. W. Saris, A. J. M. Berntsen, W. F. van der Weg, L. T. Sealy, R. C. Barklie, G. Krötz, and G. Müller, J. Appl. Phys. **75**, 7266 (1994).

[22] J. S. Custer, M. O. Thompson, D. C. Jacobson, J. M. Poate, S. Roorda, W. C. Sinke, and F. Spaepen, Appl. Phys. Lett. **64**, 437 (1994).

[23] C. A. Volkert, J. Appl. Phys. **74**, 7107 (1993).

[24] D. L. Williamson, S. Roorda, M. Chicoine, R. Tabti, P. A. Stolk, S. Acco, and F. W. Saris, Appl. Phys. Lett. **67**, 226 (1995).

[25] *Small Angle X-ray Scattering*, edited by O. Glatter and O. Kratky (Academic, New York, 1982).

[26] V. Gerold, in *Small-Angle X-Ray Scattering*, edited by H. Brumeberger (Gordon and Breach, New York, 1967), p. 277.

[27] M. H. Brodsky, M. Cardona, and J. J. Cuomo, Phys. Rev. B **16**, 3556 (1977).

[28] A. A. Langford, M. L. Fleet, and A. H. Mahan, Solar Cells **27**, 373 (1989).

[29] C. Herring and N. M. Johnson, in *Hydrogen in Semiconductors*, edited by J. I. Pankove and N. M. Johnson, Semiconductors and Semimetals Vol. 34 (Academic, San Diego, 1991), p. 279.

[30] G. L. Olson and J. A. Roth, in *Handbook of Crystal Growth*, edited by D. T. J. Hurle (Elsevier/North-Holland, Amsterdam, 1994), Vol. 3, p. 255.

[31] J. C. Oberlin, A. C. Chami, E. Ligeon, and C. Prunier, Nucl. Instrum. Methods Phys. Res. Sect. B **19/20**, 462 (1987).

[32] A decrease of a factor of 2 in the growth rate for H concentrations of $\sim3\times10^{19}$ cm^{-3} and above was observed in Refs. 30 and 31 relative to the unhydrogenated a-Si. This is in agreement with the results concerning the LH sample, where the reduction in growth rate compared with the pure a-Si is about a factor of 2. It is to be noted that in the mentioned experiments the SPE rate was observed to be only weakly dependent on H concentration from 3×10^{19} to 1.5×10^{20} cm^{-3}. At the H concentrations studied in the present work, a clear difference in thickness of the regrown layer is seen such that that of the HH sample is substantially smaller than that of the LH sample.

[33] D. L. Williamson, S. Roorda, M. Chicoine, R. Tabti, P. A. Stolk, S. Acco, and F. W. Saris, in a more complete version of Ref. 24, including structural simulation calculations of diffuse SAXS (unpublished).
[34] L. H. Schwartz and J. B. Cohen, *Diffraction from Materials* (Springer, Berlin, 1987), p. 402.
[35] A. Guiner and G. Fournet, *Small-Angle Scattering of X-Rays* (Wiley, New York, 1955).
[36] G. Lucovsky, J. Non-Cryst. Solids **76**, 173 (1985).
[37] W. B. Pollard and G. Lucovsky, Phys. Rev. B **26**, 3172 (1982).
[38] G. Lucovsky and W. B. Pollard, in *The Physics of Hydrogenated Amorphous Silicon II*, edited by J. D. Jannopolus and G. Lucovsky (Springer, Berlin, 1984), p. 301.
[39] H. Shanks, C. J. Fang, L. Ley, M. Cardona, F. J. Demond, and S. Kalbitzer, Phys. Status Solidi **100**, 43 (1980).
[40] Y. F. Chen, Solid State Commun. **71**, 1127 (1989).
[41] K. K. Gleason, M. A. Petrich, and J. A. Reimer, Phys. Rev. B **36**, 3259 (1987).
[42] J. Daey Owens and R. E. I. Schropp, in *Amorphous Silicon Technology–1995* (Ref. 10), p. 419.
[43] H.-G. Haubold and D. Martinsen, J. Appl. Crystallogr. **11**, 592 (1978).
[44] S. Chattopadhyay, S. N. Sharma, R. Banerjee, D. M. Bhusari, S. T. Kshirsagar, Y. Chen, and D. L. Williamson, J. Appl. Phys. **76**, 5208 (1994).
[45] K. F. Heidemann, M. Gruner, and E. Kaat, Radiat. Eff. **82**, 103 (1984).
[46] N. W. Ashcroft and J. Lekner, Phys. Rev. **145**, 83 (1966).
[47] C. G. Vonk, J. Appl. Crystallogr. **9**, 433 (1976).
[48] R. Triolo, E. Caponetti, and S. Spooner, Phys. Rev. B **39**, 4588 (1989).
[49] Y. J. Chabal and C. K. N. Patel, Rev. Mod. Phys. **59**, 835 (1987).
[50] H. J. Stein and P. S. Peercy, Appl. Phys. Lett. **34**, 604 (1979); Phys. Rev. B **22**, 6233 (1980).
[51] G. N. van den Hoven, Z. N. Liang, L. Niesen, and J. S. Custer, Phys. Rev. Lett. **68**, 3714 (1992).
[52] Y. K. Park, S. K. Estreicher, C. W. Myles, and P. A. Fedders, Phys. Rev. B **52**, 1718 (1995).
[53] W. E. Carlos and P. C. Taylor, Phys. Rev. B **25**, 1435 (1982).
[54] H. v. Löhneyesn, H. J. Schink, and W. Beyer, Phys. Rev. Lett. **52**, 549 (1984).
[55] J. E. Graebner, B. Golding, L. C. Allen, D. K. Biegelsen, and M. Stutzmann, Phys. Rev. Lett. **52**, 553 (1984).
[56] J. B. Boyce, S. E. Ready, M. Stutzmann, and R. E. Norberg, J. Non-Cryst. Solids **114**, 211 (1989).
[57] A. J. M. Berntsen, Ph.D. thesis, Utrecht University, 1993.
[58] R. A. Street, Physica B **170**, 69 (1991).
[59] P. V. Santos, N. M. Johnson, R. A. Street, M. Hack, R. Thompson, and C. C. Tsai, Phys. Rev. B **47**, 10 244 (1993).
[60] D. E. Carlsson and C. W. Magee, Appl. Phys. Lett. **33**, 81 (1978).
[61] W. Beyer and H. Wagner, J. Appl. Phys. **53**, 8745 (1982).
[62] K. Böhringher, X. H. Liu, and S. Kalbitzer, J. Phys. C **16**, L1187 (1983).
[63] W. Beyer (private communication).
[64] S. Coffa and J. M. Poate, Appl. Phys. Lett. **59**, 2296 (1991).
[65] G. Luckovsky, Z. Zing, Z. Lu, D. R. Lee, and J. L. Whitten, J. Non-Cryst. Solids **182**, 90 (1995).
[66] M. Nakamura, T. Ohno, K. Miyata, N. Konishi, and T. Suzuki, J. Appl. Phys. **65**, 3061 (1989).
[67] A. Carnera (private communication).
[68] A. A. Langford, M. L. Fleet, B. P. Nelson, W. A. Lanford, and N. Maley, Phys. Rev. B **45**, 13 367 (1992).
[69] M. A. Petrich, K. K. Gleason, and J. A. Reimer, Phys. Rev. B **36**, 9722 (1987).
[70] S. Mitra, K. K. Gleason, H. Jia, and J. Shinar, Phys. Rev. B **48**, 2175 (1993).
[71] M. Kemp and H. M. Branz, Phys. Rev. B **52**, 13 946 (1995).
[72] A. H. Mahan, E. J. Johnson, R. S. Crandall, and H. M. Branz, in *Amorphous Silicon Technology–1995* (Ref. 10), p. 413.
[73] C. C. Tsai and H. Fritzsche, Solar Energy Mater. **1**, 29 (1979).
[74] W. Beyer, in *Tetrahedrally-Bonded Amorphous Semiconductors*, edited by D. Adler and H. Fritzsche (Plenum, New York, 1985), p. 129.
[75] S. Mantl, Mater. Sci. Rep. **8**, 1 (1992).
[76] J. E. Graebner, L. C. Allen, and B. Golding, Phys. Rev. B **31**, 904 (1985).
[77] K. M. Jones (private communication).
[78] P. C. Taylor, W. D. Ohlsen, C. Lee, and E. D. van der Heiden, in *Hydrogen in Disordered and Amorphous Solids*, edited by G. Bambakidis and R. C. Bowman (Plenum, New York, 1986), p. 91.
[79] R. Rüther and J. Livingstone, Thin Solid Films **251**, 30 (1994).
[80] A. Polman, D. C. Jacobson, S. Coffa, J. M. Poate, S. Roorda, and W. Sinke, Appl. Phys. Lett. **57**, 1230 (1990).
[81] S. Coffa, J. M. Poate, D. C. Jacobson, and A. Polman, Appl. Phys. Lett. **58**, 2916 (1991).
[82] H. M. Branz, S. Asher, B. P. Nelson, and M. Kemp, in *Amorphous Silicon Technology—1993*, edited by E. A. Schiff, M. J. Thompson, A. Madan, K. Tanaka, and P. G. Lecomber, MRS Symposia Proceedings. No. 297 (Materials Research Society, Pittsburgh, 1993), p. 279.
[83] W. B. Jackson, N. H. Nickel, N. M. Johnson, F. Pardo, and P. V. Santos, in *Amorphous Silicon Technology—1994*, edited by E. A. Schiff, M. Hack, A. Madan, M. Powell, and A. Matsuda, MRS Symposia Proceedings No. 336 (Materials Research Society, Pittsburgh, 1994), p. 311.
[84] S. Coffa, F. Priolo, and A. Battaglia, Phys. Rev. Lett. **70**, 3756 (1993).
[85] C. N. Waddel, W. G. Spitzer, J. E. Fredrikson, G. H. Hubler, and T. A. Kennedy, J. Appl. Phys. **55**, 4361 (1984).
[86] N. H. Nickel and W. B. Jackson, Phys. Rev. B **51**, 4872 (1995).
[87] G. F. Cerofolini, L. Meda, R. Balboni, F. Corni, S. Fabbroni, G. Ottaviani, R. Tonini, M. Anderle, and R. Canteri, Phys. Rev. B **46**, 2061 (1992).
[88] M. F. Beaufort, H. Garem, and J. Lépinoux, Philos. Mag. A **69**, 881 (1994).
[89] S. Romani and J. H. Evans, Nucl. Instrum. Methods Phys. Res. Sect. B **44**, 313 (1990).